

General Disclaimer

One or more of the Following Statements may affect this Document

- This document has been reproduced from the best copy furnished by the organizational source. It is being released in the interest of making available as much information as possible.
- This document may contain data, which exceeds the sheet parameters. It was furnished in this condition by the organizational source and is the best copy available.
- This document may contain tone-on-tone or color graphs, charts and/or pictures, which have been reproduced in black and white.
- This document is paginated as submitted by the original source.
- Portions of this document are not fully legible due to the historical nature of some of the material. However, it is the best reproduction available from the original submission.



Technical Memorandum 79585

Analysis of Daily Latitude Variations

(NASA-TM-79585) ANALYSIS OF DAILY LATITUDE
VARIATIONS (NASA) 19 F HC A02/MF A01
CSSL 04A

N78-30757

Unclas
G3/46 29339

Michael A. Graber

July 1978

National Aeronautics and
Space Administration

Goddard Space Flight Center
Greenbelt, Maryland 20771

TM 79585

ANALYSIS OF DAILY LATITUDE

VARIATIONS

**Michael A. Graber
Geodynamics Branch, Code 921
Goddard Space Flight Center
Greenbelt, Maryland 20771, U. S. A.**

July 1978

**GODDARD SPACE FLIGHT CENTER
Greenbelt, Maryland**

ANALYSIS OF DAILY LATITUDE
VARIATIONS

Michael A. Graber
Geodynamics Branch, Code 921

ABSTRACT

The daily latitude measurements of the International Polar Motion Service are analyzed. The results indicate that the annual polar oscillation is probably due to local phenomena with amplitudes varying from 0".05 to 0".15. Within the resolution of the residuals (150 cm), there is no indication of the sharp changes which might be associated with earthquake effects. Then, applying Schuster's test to a periodogram of the residuals indicates that there are probably several processes occurring at amplitudes between 0".007 and 0".03 whose solution awaits a more precise measurement technique.

ANALYSIS OF DAILY LATITUDE VARIATIONS

The position of the rotation axis in an earth-fixed coordinate system has been monitored for over 80 years. The most notable phenomenon identified in this data has been the Chandler wobble. A review of past analyses of the pole position data can be found in Stacey [1977] and in Munk and MacDonald [1960]. A discussion of the optical observing technique is in Melchior [1957]. These analyses have traditionally been based upon the mean x- and y-coordinates of the pole as reported by the International Polar Motion Service (IPMS) (previously called the International Latitude Service) and the Bureau International de l'Heure (BIH) for various time intervals. In this analysis it was decided to go back one step and utilize the IPMS latitude measurements, rather than the reported pole positions.

Four years of daily latitudes as reported in the Monthly Notes of the IPMS are analyzed. The data base is composed of 3788 daily latitude measurements (weighted by the number of star pair observations during that day) from 1971.0 to 1975.0 for the five primary IPMS stations: Gaithersburg, Ukiah, Mizusawa, Kitab, and Carloforte. Table 1 provides a summary of this data.

The data do not form an equally spaced time series and are analyzed through a general least-squares procedure. The condition equation upon which the least-squares analysis was based is given by equation 1.

Table 1
Composition of the latitude data base

	Daily latitudes in 1461 days	Total star pairs observed
Gaithersburg	1001	12042
Ukiah	887	13603
Mizusawa	626	5588
Kitab	497	7948
Carloforte	777	9952

$$\phi_i(t) = \Phi_i + A_i (\text{ANNUAL}) \cos [2\pi ft + \psi_i - \lambda_i] + X(t) \cos [\lambda_i] + Y(t) \sin [\lambda_i] \quad (1)$$

Each latitude measurement $\phi_i(t)$ (where i refers to the particular observing station and t designates the time of observation) was assumed to be a function of four terms. The first is a constant station latitude Φ_i . The second represents an individual annual oscillation for each station (where f is the known annual frequency). An annual amplitude A_i and phase ψ_i are derived for each station. The annual component of the latitude data was modelled by individual station sinusoids rather than two circularly polarized common terms because preliminary analysis indicated that individual annual effects were as large as the predicted amplitude of the common annual term. The data would not have been properly modelled by only common terms for the annual oscillation. The $X(t)$ and $Y(t)$ terms in equation 1 represent the common processes in the polar motion such as the Chandler wobble.

The λ_1 is the longitude of the observing station. Values for these longitudes were taken from IPMS publications. This longitude is an angle increasing in a counterclockwise direction from Greenwich. It is present in the argument of the annual term in equation 1 to give the annual phases a common origin.

If the Chandler wobble were the only periodic process occurring, then $X(t)$ and $Y(t)$ would be given by equation 2.

$$\begin{aligned} X_0(t) &= A \cos [2\pi t/\text{Period} + \text{Phase}] \\ Y_0(t) &= A \sin [2\pi t/\text{Period} + \text{Phase}] \end{aligned} \tag{2}$$

The x-axis points toward Greenwich, and the y-axis toward 90° E longitude. This would add three parameters to the least-squares analysis: an amplitude, period, and phase. Thus in this preliminary configuration, the least-squares analysis fits eighteen parameters: five average latitudes, five pairs of annual amplitude and phase, and the three Chandler parameters.

The least-squares technique is iterative and was repeated until all parameters changed by no more than 0.002 times their associated standard error. The solution was then considered to have converged. The results of this 18 parameter fit are given in Table 2. The phase angles are given relative to Greenwich at 1971.0 with the angles increasing in the counterclockwise direction. In all cases, these phases are included in the argument of the sine or cosine with a positive sign. The correlation matrix associated with this solution appears in Table 3.

Table 2

Values obtained for the 18 parameters in the preliminary analysis.
The number in parentheses is the square root of the variance.

Average latitude	G	39° 8'	13''3755	(0''0034)
	U	39° 8'	12''3659	(0''0034)
	M	39° 8'	3''3520	(0''0051)
	K	39° 8'	1''6647	(0''0047)
	C	39° 8'	9''0170	(0''0041)
Annual amplitude and phase	G		0''1112	(0''0051)
			96.8°	(3.6°)
	U		0''1391	(0''0057)
			132.3°	(2.6°)
	M		0''1343	(0''0076)
		93.1°	(3.6°)	
Chandler wobble	K		0''0515	(0''0066)
			72.2°	(8.7°)
	C		0''0442	(0''0057)
		86.8°	(9.3°)	
Chandler wobble	amplitude		0''1338	(0''0038)
	period		431.0 d.	(2.4 d.)
	phase		112.6°	(3.6°)

The values in Table 2 determined for the station latitudes disagree with those published by the IPMS [Yumi, 1975], which are based on the CIO coordinate system and are given as

Gaithersburg	39° 8'	13''202
Ukiah		12''096
Mizusawa		3''602
Kitab		1''850
Carloforte		8''941

Table 3
Correlation matrix associated with the 18 parameter solution. The parameters are listed here, 1 through 18, in the same order as in Table 2.

1	1.																	
2	.0	1.																
3	.0	.0	1.															
4	.0	.0	.0	1.														
5	.0	.0	.0	.0	1.													
6	.0	.0	.0	.0	.0	1.												
7	.0	.0	.0	.1	.1	.0	1.											
8	.0	.0	.0	.0	.0	.1	.4	1.										
9	.0	.2	.0	.0	.1	.0	.5	.3	1.									
10	.0	.0	-.1	.0	.0	.0	.0	.0	.0	1.								
11	.0	.0	.0	.0	.0	.0	.4	.3	.4	.0	1.							
12	.0	.0	.0	.3	.0	.0	-.2	-.1	-.2	.0	-.1	1.						
13	.0	.0	.0	-.2	.0	.0	.4	.4	.4	.0	.3	-.2	1.					
14	.0	.0	.0	.0	-.1	.1	.0	.0	.0	.1	.0	.0	.0	1.				
15	.0	.0	.0	.0	-.2	.0	.5	.4	.4	.0	.4	-.2	.4	.0	1.			
16	.0	-.1	-.1	.1	.1	.0	.6	.5	.5	.0	.5	-.2	.5	.0	.5	1.		
17	.0	.1	.0	-.1	-.1	.0	-.7	-.6	-.6	.0	-.6	.2	-.6	.0	-.6	-.6	1.	
18	-.1	.0	.0	.0	-.1	-.1	-.7	-.6	-.6	.0	-.5	.2	-.6	-.1	-.6	-.6	.9	1.
1	2	3	4	5	6	7	8	9	10	11	12	13	14	15	16	17	18	

The differences are primarily due to the long term secular drift of the pole towards North America and to short term effects which cause the figures traced out by the wobble to be non-concentric. There might also be some differences due to varying data analysis methods. To keep the differences in perspective, it should be recalled that 0.'01 is equal to 31 cm. on the earth's surface.

After performing the 18 parameter analysis, the latitude residuals were converted to pole positions and were fit to a series of connected line segments, each 20 days long. The x- and y-coordinates of the connection points were found by weighted least squares. The power spectrum of this residual time

series of connection points was determined by standard Fourier analysis.

This spectrum is displayed in Figure 1.

The peaks at -1.25 , $+1.25$, and $+2.50$ cycles per year (cpy) appeared interesting,

and it was decided to repeat the least squares analysis to include these terms.

Preliminary investigation indicated that the -1.25 and $+1.25$ peaks can be described by a linear oscillation of the pole position along the x-axis (the Greenwich meridian).

Therefore, the condition equation was modified so that the

$X(t)$ and $Y(t)$ common terms were given by equation 3 (at the bottom of page 7).

The results of this 24 parameter fit are given in Table 4, and the corresponding

correlation matrix in Table 5.

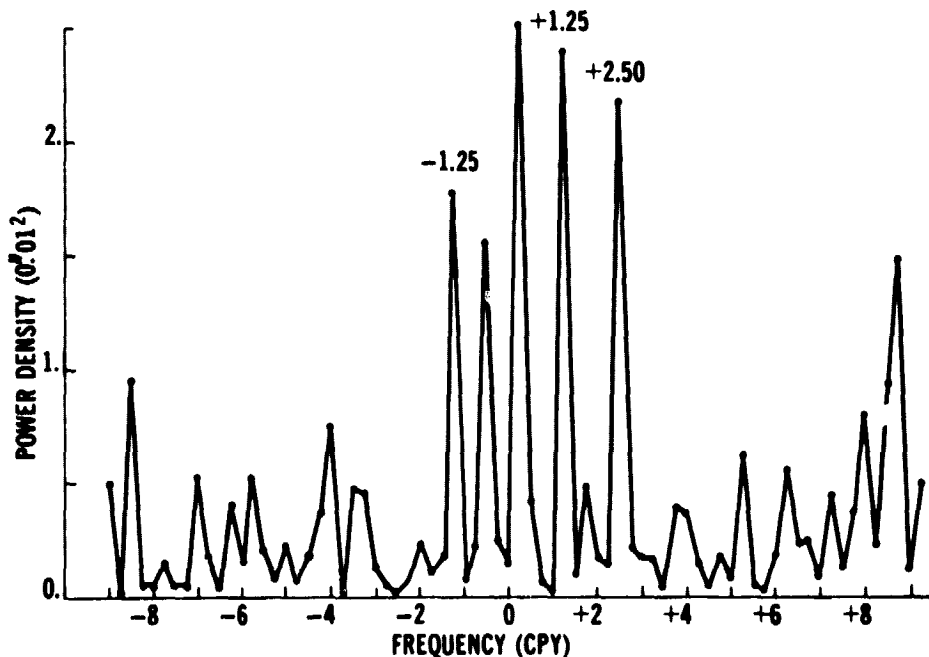


Figure 1. Power spectrum by Fourier analysis of the residual time series from the 18 parameter fit.

Table 4
Values obtained for the 24 parameters in the second least-squares analysis. The number in parentheses is the square root of the variance.

Average latitude	G	39° 8'	13''3759	(0''0034)
	U	39° 8'	12''3653	(0''0034)
	M	39° 8'	3''3514	(0''0050)
	K	39° 8'	1''6643	(0''0046)
	C	39° 8'	9''0157	(0''0040)
Annual amplitude and phase	G		0''1147	(0''0052)
			100.7°	(3.9°)
	U		0''1489	(0''0073)
			132.7°	(2.7°)
	M		0''1409	(0''0086)
		95.8°	(3.7°)	
Chandler wobble	K		0''0513	(0''0064)
			84.8°	(10.1°)
	C		0''0556	(0''0082)
			101.5°	(8.8°)
	amplitude		0''1411	(0''0047)
period		427.7 d.	(2.6 d.)	
phase		105.5°	(3.9°)	
1.25 cpy term	amplitude		0''0304	(0''0045)
	period		303.9 d.	(7.6 d.)
	phase		138.5°	(24.0°)
2.50 cpy term	amplitude		0''0129	(0''0024)
	period		148.1 d.	(1.5 d.)
	phase		140.7°	(20.8°)

$$X_1(t) = X_0(t) + A(1.25) \cos[2\pi t/\text{Period}(1.25) + \text{Phase}(1.25)]$$

$$+ A(2.50) \cos[2\pi t/\text{Period}(2.50) + \text{Phase}(2.50)]$$

$$Y_1(t) = Y_0(t) + A(2.50) \sin[2\pi t/\text{Period}(2.50) + \text{Phase}(2.50)] \quad (3)$$

Table 5
 Correlation matrix associated with the 24 parameter solution. The parameters
 are listed here, 1 through 24, in the same order as in Table 4.

1	1.																									
2	.0	1.																								
3	.0	.0	1.																							
4	.0	.0	.0	1.																						
5	.0	.0	.0	.0	1.																					
6	.0	.6	.0	.0	.0	1.																				
7	.0	.0	.0	.1	.1	.1	1.																			
8	.0	.0	.0	.0	.0	.2	.4	1.																		
9	.0	.2	.0	.0	.0	.1	.5	.5	1.																	
10	.0	.0	.0	.0	.0	.1	.0	.3	.1	1.																
11	.0	.0	.0	.1	.0	.1	.5	.3	.4	.0	1.															
12	.0	.0	.0	.2	.0	.0	-.1	.0	-.1	.1	-.1	1.														
13	.0	.0	.0	-.2	.0	.2	.5	.6	.5	.2	.4	-.1	.3	1.												
14	.0	.0	.0	.0	-.2	.2	.1	.5	.2	.4	.0	.1	.3	.1.												
15	.0	.0	.0	.0	-.2	.2	.5	.5	.6	.2	.4	-.1	.5	.3	1.											
16	.0	-.1	-.1	.1	.0	.2	.7	.6	.6	.2	.5	-.1	.6	.3	.7	1.										
17	.0	.0	.0	-.1	-.1	-.2	-.8	-.6	-.7	-.1	-.6	.1	-.7	-.2	-.7	-.7	1.									
18	-.1	.0	.0	.0	.0	-.3	-.7	-.7	-.6	-.2	-.6	.0	-.7	-.3	-.7	-.7	.9	1.								
19	.0	.0	.0	.0	.0	.2	.2	.4	.2	.3	.1	.0	.3	.5	.3	.3	-.3	-.3	1.							
20	.0	.0	.0	.0	.0	.2	.0	.5	.2	.5	-.1	.1	.3	.7	.3	.2	-.1	-.2	.4	1.						
21	.0	.0	.0	.0	.0	.2	.1	.5	.3	.4	.0	.0	.4	.6	.4	.3	-.2	-.2	.4	.9	1.					
22	.0	.0	.0	.0	.0	.0	.0	.0	.0	.0	.0	.0	.0	.0	.0	.0	.0	.0	.0	.0	1.					
23	.0	.0	.0	.0	.0	.1	.0	.0	-.1	.1	.0	.0	.0	.0	.0	.0	.0	.0	.0	.1	.1	.0	1.			
24	.0	.0	.0	.0	.0	.1	.0	.1	.0	.1	.0	.0	.1	.0	.0	.0	.0	.0	.0	.1	.1	.0	.9	1.		
1	2	3	4	5	6	7	8	9	10	11	12	13	14	15	16	17	18	19	20	21	22	23	24			

The residual analysis was performed and the connection point coordinates for this 24 parameter fit are displayed in Figure 2, with the associated power spectrum in Figure 3.

The points in Figure 2 were displayed in an attempt to determine whether earthquake effects could be observed in the polar motion. Earthquakes are known to change the moment of inertia of the earth through their redistribution of the earth's mass. However it is not known whether this change is sufficiently large to be observed. In Figure 2, the effect would be seen as a "step-function" in the X or Y time series. There does not appear to be such an effect in the four years of data utilized here.

It is interesting to consider identifying the points in the periodogram in Figure 3 which might correspond to real periodic phenomena in the pole position data. To do this, Schuster's test is utilized [see Fisher, 1929]. In an unsmoothed periodogram based completely on random noise processes, the points will be distributed so that the number of points above any positive power C is proportional to $\exp(-\lambda C)$, where λ is a positive constant determined by the data. Figure 4a displays the behavior of all 73 points in Figure 3. The ordinate is the natural logarithm of the number of points, so exponential behavior will be shown as a straight line. If a small number of points represent signal, the low power end of the curve will still appear as a straight line since the small

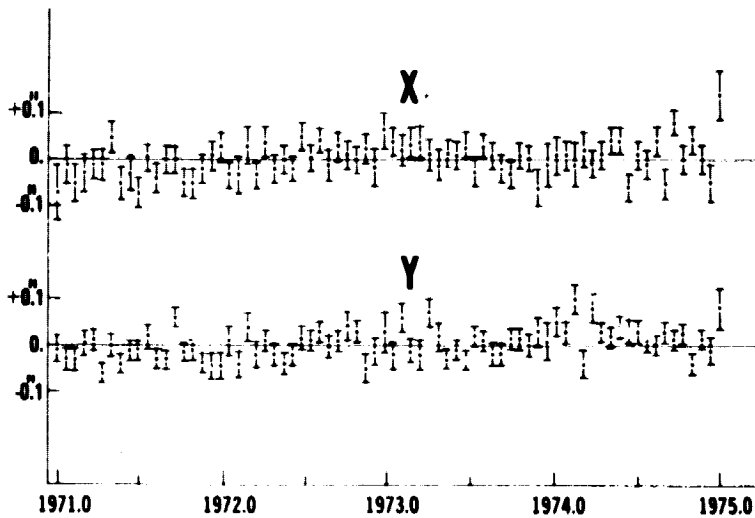


Figure 2. Coordinate values with standard errors for the connection points of the line segments which were fit to the residuals of the 24 parameter least-squares analysis. The x-axis is positive toward's Greenwich; the y-axis is positive toward 90°E longitude.

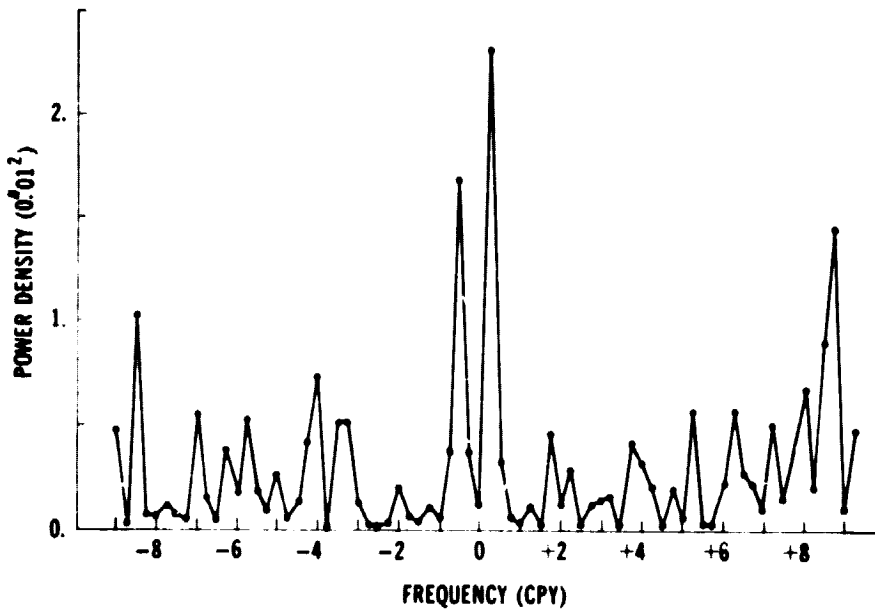


Figure 3. Power spectrum by Fourier analysis of the connection point coordinates which are displayed in Figure 2. Ideally this figure would be identical to Figure 1 after removal of that figure's labelled peaks.

additive constant will not have a large effect. However, the signal points would cause the tail end of the curve to rise as is seen in Figure 4a. To make a rough determination of the number of signal points present, four arbitrary points from the highest power subset (0.45×0.01^2 to infinity) were removed, and the graph was replotted in Figure 4b. The tail has been lowered, but still indicates additional signal. A further four points from the same subset were removed, reducing the number of periodogram points to 65, and Figure 4c was plotted. This time the graph was found to follow an excellent straight line, indicating that the remaining points represent noise processes.

The constant λ determined from Figure 4c for Schuster's test is $4.6 \times (0.01^2)^{-1}$. The inverse of this constant is equal to twice the variance of the underlying random process (in this case, the 20 day residual connection points), producing a variance of $(1/3 \times 0.01)^2$. This variance is associated with the time series of connection points and does not incorporate the least-squares standard deviations indicated in Figure 2.

Table 6 presents the conclusions which can be derived from Figure 4. The significance of this table can be seen by studying column d. For example, it indicates that if in Figure 3 a point having a value between 0.45×0.01^2 and 0.60×0.01^2 is chosen arbitrarily, then the probability is 0.56 that this point represents a non-random fluctuation of the pole. Most notably, the two points in Figure 3 which are above 1.55×0.01^2 each have a probability of 0.98 that they represent

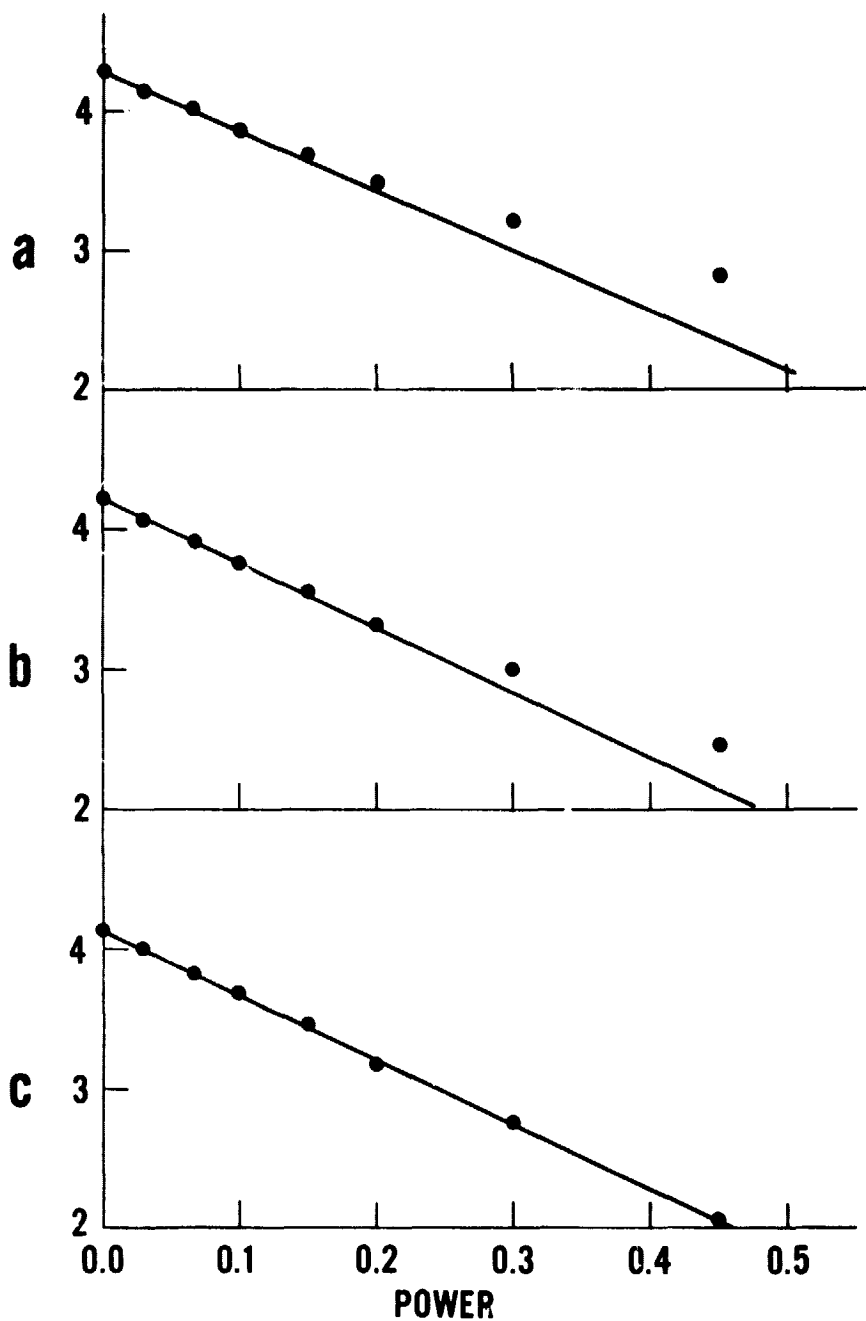


Figure 4. The number of periodogram points in Figure 3 above a given power is determined and the natural logarithm of that number plotted. Figure 4a represents the entire set of 73 periodogram points; Fig. 4b has four points removed; Fig. 4c has eight removed.

Table 6

Column a presents the actual number of periodogram points per power interval in Figure 3. Column b indicates the number of points predicted for the power interval by Figure 4c, where $\lambda = 4.6 \times (0.01^2)^{-1}$. These points are interpreted as being due to noise processes. Column c gives the difference between columns a and b and is interpreted as the number of points in the power interval which might represent real periodic phenomena in the pole position data. Column d gives the probability that an arbitrary periodogram point in the power interval is "signal".

Power Interval (0.01^2)	a	b	c	d
0.0 - .15	33	33	0	.0
.15 - .30	16	16	0	.0
.30 - .45	8	8	0	.0
.45 - .60	9	4	5	.56
.60 - 1.55	5	3.95	1.05	.21
1.55 - ∞	<u>2</u>	<u>0.05</u>	<u>1.95</u>	<u>.98</u>
Total	73	65	8	

real periodic phenomena. The power at the semi-annual frequencies (approximately 0.25×0.01^2) is well within the noise region. Any attempt to resolve the semi-annual constituents from this data would probably be meaningless.

Another test for the accuracy of the residual power spectrum would be to compare the amplitudes predicted for the 1.25 and 2.50 cpy terms by Figure 1 which is a periodogram analysis with the values determined by the 24 parameter least-squares fit as shown in Table 4. The amplitude of the 1.25 linear term is determined by summing the square roots of the peak values for -1.25 and +1.25 cpy. This value is 0.0287 and is within one-half of a standard deviation from the least squares value 0.0304. The amplitude of the 2.50 cpy term is 0.0147 in

Figure 1 and 0.'0129 in Table 4. Thus the residual analysis of the connection points appears to be as accurate as a general least-squares procedure based on the entire data set and seems to provide an accurate display of the power distribution of the IPMS latitude data.

This analysis has taken a group of data which have been significantly underutilized, namely the IPMS daily latitude observations, and several important features of the motion of the pole have emerged. The annual oscillations at the individual observing stations are seen to vary from 0.'05 to 0.'15 in amplitude with sizable variations in phase. Previous analyses which purport to have determined an annual oscillation common to all the stations are probably missing the fact that these terms are most likely due to purely local phenomena. Secondly, a plot of the least-squares residual analysis in Figure 2 shows no sign of earthquake effects. This does not mean that the effects are absent, but rather that they are smaller than the scale of that figure (approximately 0.'05 or 150 cm.). And finally, Schuster's test gives a method for identifying the presence or absence of physical processes in the residuals. There are still several unsuspected processes occurring at amplitudes between $0.7 \times 0.'01$ and $3 \times 0.'01$ whose solution awaits a more precise measurement technique.

REFERENCES

- Fisher, R. A., Tests of Significance in Harmonic Analysis, Proc. Royal Soc. London A, 125, 54-59, 1929.
- Melchior, P. J., Latitude Variation, in Physics and Chemistry of the Earth, vol. 2, edited by L. H. Ahrens et al., pp. 212-243, Pergamon Press, London, 1957.
- Munk, W. H., and G. J. F. MacDonald, The Rotation of the Earth, Cambridge University Press, London, 1960.
- Stacey, F. D., Physics of the Earth, 2nd edition, Wiley, New York, 1977.
- Yumi, S., Annual Report of the International Polar Motion Service for the Year 1973, Mizusawa, 1975.